This is an open access article published under an ACS AuthorChoice License, which permits copying and redistribution of the article or any adaptations for non-commercial purposes.

ACS OMEGA

Article

http://pubs.acs.org/journal/acsodf

# pH and Thermal Dual-Responsive Nanoparticles for Controlled Drug Delivery with High Loading Content

Yang Zheng, Lei Wang, Lin Lu, Qian Wang, and Brian C. Benicewicz*

Department of Chemistry and Biochemistry, University of South Carolina, Columbia, South Carolina 29208, United States

Supporting Information

**ABSTRACT:** A pH and thermal dual-responsive nanocarrier with silica as the core and block copolymer composed of poly(methacrylic acid) (PMAA) and poly(*N*-isopropylacrylamide) (PNIPAM) as the shell was prepared by surface-initiated reversible addition−fragmentation chain-transfer (SI-RAFT) polymerization. The resulting $SiO_2$-PMAA-*b*-PNIPAM particles dispersed individually in an aqueous solution at a high pH and a low temperature but reversibly agglomerated under acidic conditions or at elevated temperatures. These dual-responsive nanoparticles were used as carriers to deliver the model drug doxorubicin (DOX) with unusually high entrapment efficiency and loading content, which is due to the small size (15 nm), light weight of the cores, and high graft density (0.619 chains/nm$^2$) achieved by SI-RAFT polymerization. The release rate was controlled by both the pH and temperature of the surrounding medium. Moreover, these particles selectively precipitated at acidic conditions with increased temperature, which may enhance their ability to accumulate at tumor sites. Cytotoxicity studies demonstrated that DOX-loaded nanoparticles are highly active against Hela cells and more effective than free DOX of an equivalent dose. A cellular uptake study revealed that $SiO_2$-PMAA-*b*-PNIPAM nanoparticles could successfully deliver DOX molecules into the nuclei of Hela cells. All these features indicated that $SiO_2$-PMAA-*b*-PNIPAM nanoparticles are a promising candidate for therapeutic applications.

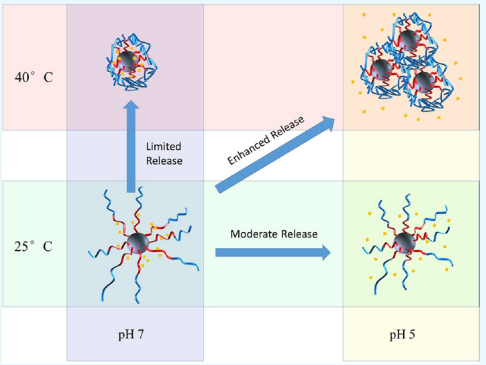


## INTRODUCTION

Polymer-grafted nanoparticles have gained significant attention because of their wide application in materials science, bioimaging, and drug delivery.[1−5] The surface-initiated reversible addition−fragmentation chain-transfer (SI-RAFT) polymerization technique has been developed as a robust method to graft polymers from silica surfaces with a predetermined density and controlled molecular weights.[6−8] A variety of polymers with well-defined architectures (homopolymer, block copolymer, bimodal brushes) have been successfully grafted to demonstrate the effectiveness of this method.[9−12] Stimuli-responsive polymers are materials that can adapt to environmental changes like pH, temperature, ionic strength, and light.[13−18] Poly(methacrylic acid) (PMAA) and poly(*N*-isopropylacrylamide) (PNIPAM) are typical stimuli-responsive polymers that have been widely studied. PMAA chains change conformation in water in response to pH changes. Under basic conditions, the carboxylic groups along the polymer chains are deprotonated, creating charges that make the polymer swell in water. At low pH (<5), carboxylic groups are protonated, making the chains hydrophobic and adapt a collapsed conformation.[19,20] Comparatively, PNIPAM chains can perform similar conformational transformations in response to temperature. Below the lower critical solution temperature (LCST), PNIPAM chains stretch out and swell in aqueous solution. A phase transition occurs at temperatures above LCST, when the chains become hydrophobic and collapse into a condensed conformation.[21]

Grafting stimuli-responsive polymers onto inorganic nanoparticles is an interesting topic because the combined assembly could exhibit properties inherent in both the inorganic cores and grafted polymers. A common application of these core−shell structures is the controlled delivery of active species into biological targets. For example, Ma et al. prepared magnetic colloid nanocrystal clusters covered with cross-linked poly(acrylic acid) that conjugated doxorubicin (DOX) and released them upon reduction in pH,[22] and Xu et al. synthesized multifunctional carriers with silicon as the core and a biocompatible block copolymer as the shell. The release rate was found to be regulated by both the pH and chain length of the outer block.[23] However, the drug-loading (DL) contents and entrapment efficiency (EE) were relatively low compared to those of pure polymer systems presumably because of the high weight content of the cores and low graft density of polymers achieved by the "grafting to" process.

Our group has reported SI-RAFT polymerization of methacrylic acid (MAA) from 15 nm silica nanoparticles.[19,24] This direct "grafting from" strategy offers a convenient way to achieve high graft densities and subsequently a high polymer

Received: June 6, 2017
Accepted: June 28, 2017
Published: July 11, 2017

 © 2017 American Chemical Society 

DOI: 10.1021/acsomega.7b00367
ACS Omega 2017, 2, 3399−3405

content. On the basis of this work, a rationally designed core−shell drug delivery system is described using 15 nm silica nanoparticles as cores and PMAA-*b*-PNIPAM block copolymer as shells. PMAA, as the inner block, was used to conjugate with drug molecules through electrostatic attraction forces. The PNIPAM outer block not only introduced temperature responsiveness, but also helped to prevent premature drug leaking. These nanocarriers exhibited unusually high EE and loading content (LC) when using DOX as a model drug. The drug release rate was found to be affected by both pH and temperature. Specifically, the release rate was enhanced at acidic pH and high temperature, which is the typical environment of tumor cells.[21] It is also worth noting that these nanoparticles are well dispersed at low temperatures but self-assembled into clusters and eventually precipitated at elevated temperatures, which may enhance their ability to accumulate around tumor cells.

## EXPERIMENTAL SECTION

**Materials.** All chemicals were obtained from Acros or Fisher and used as received unless otherwise specified. *N*-Isopropylacrylamide (NIPAM) was obtained from TCI and recrystallized twice from hexane to remove inhibitor. MAA was purified by passing through an activated neutral alumina column. AIBN was recrystallized from methanol and dissolved in dimethylformamide (DMF) solution at a concentration of 10 mmol/L.

**Instrumentation.** $^1$H NMR (Bruker ARX 300/ARX 400) spectroscopy was conducted using $CD_3OD$ as the solvent. Molecular weights and polydispersity index (PDI) were determined using a gel permeation chromatography with a 515 HPLC pump, a 2410 refractive index detector, and three Styragel columns. The columns consist of HR1, HR3, and HR4 in the effective molecular weight ranges of 100−5000, 500−30 000, and 5000−500 000, respectively. THF was used as an eluent at 30 °C, and the flow rate was adjusted to 1.0 mL/min. Molecular weights were calibrated with poly(methyl methacrylate) standards obtained from Polymer Laboratories. DLS characterizations were conducted using a Zetasizer Nano ZS90 from Malvern. Infrared spectra were obtained using a BioRad Excalibur FTS3000 spectrometer. Optical spectroscopy was conducted by measuring the transmittance at 300 nm using a PerkinElmer Lambda 4C UV−vis spectrometer.

**SI-RAFT Polymerization of MAA from 4-Cyanopentanoic Acid Dithiobenzoate (CPDB)-Anchored Silica Nanoparticles.** CPDB-anchored 15 nm silica nanoparticles were prepared according to the literature.[1] For a typical reaction, 400 mg of CPDB-anchored silica nanoparticles (0.619 chains/nm$^2$, 146.7 $\mu$mol/g), 5.05 g of MAA (58.7 mmol), and 400 mg of trioxane were mixed in 12 mL of DMF and subjected to sonication for 2 min. AIBN solution (1.17 mL, 10 mmol/L) in DMF was then added. The above mixture was transferred to a Schlenk tube and degassed by three freeze−pump−thaw cycles, backfilled with nitrogen, and placed in an oil bath of 65 °C for 2.5 h. The polymerization was stopped by quenching in an ice bath. The resulting solution was washed twice with diethyl ether to remove monomers and initiator, and the PMAA-grafted particles were redispersed in 20 mL of DMF for subsequent reaction.

**SI-RAFT Polymerization of PNIPAM-*b*-PMAA from Surface-Anchored Macroinitiator.** A 10 mL solution of PMAA-grafted silica nanoparticles with an active RAFT agent chain end was mixed with 3.22 g of NIPAM monomer, 0.58 mL of 1 mmol/L AIBN solution, and 500 mg of trioxane. The above mixture was degassed by three freeze−pump−thaw cycles and placed in an oil bath of 80 °C for 12 h. The polymerization was stopped by quenching in an ice bath.

**Preparation of DOX-Loaded $SiO_2$-PMAA-*b*-PNIPAM Particles.** A typical process to load DOX onto $SiO_2$-PMAA-*b*-PNIPAM particles is described as follows: 12 mL of 1 mg/mL DOX solution was added into a solution of 40 mg particles, and the mixture was stirred overnight under dark conditions. The DOX-loaded particles were recovered by ultracentrifugation at 20 000 rpm and 40 °C for 1 h and washed twice by deionized (DI) water to remove free DOX. All supernatant was collected and subjected to UV−vis analysis to determine the drug encapsulation efficiency (EE) and DL contents. A calibration curve of DOX in water was made as the reference. EE and DL were determined using the equations

$$\text{DL contents (\%)} = \frac{\text{weight of drug loaded}}{\text{weight of nanoparticles}} \times 100$$

$$\text{drug EE (\%)} = \frac{\text{weight of drug loaded}}{\text{weight of drug injected}} \times 100$$

**In Vitro Drug Release from DOX @ $SiO_2$-PMAA-*b*-PNIPAM.** Nanoparticles loaded with DOX were redispersed in 16 mL of DI water. The dispersion was then transferred into dialysis bags. The bags were subsequently placed in beakers of different solutions (pH 5.0 sodium acetic acid buffer or pH 7.0 phosphate-buffered saline (PBS) buffer) at different temperatures (25 or 40 °C). Each solution (2 mL) was sampled at certain periods of time and analysis using a UV−vis spectrometer was conducted to determine the amount of released DOX. All drug release data were averages of three measurements.

**Cell Culture.** Hela cells were obtained from ATCC. They were grown on standard tissue culture plastic in a 5% $CO_2$ humidified incubator at 37 °C. The cell culture medium was Dulbecco's modified Eagle's medium with 10% fetal bovine serum and 1% penicillin/streptomycin antibiotics.

**Cell Viability Assay.** Biocompatibilities of $SiO_2$-PMAA-*b*-PNIPAM nanoparticles, free DOX, and DOX-loaded nanoparticles were tested on Hela cells, and cell viability was determined by CellTiter-Blue assay. Briefly, cells were seeded on a 96-well plate at a density of $1.0 \times 10^4$ cell/well and incubated at 37 °C with 5% $CO_2$ for 24 h. Then, the cell culture medium was replaced with 100 $\mu$L of a fresh medium containing various concentrations of testing samples. After 24 h of incubation, the testing samples were removed and 10% CellTiter-Blue Reagent was added to each well and incubated for 4 h. The fluorescence was recorded on a Spectramax Gemini EM spectrophotometer with excitation and emission wavelengths of 560 and 590 nm, respectively.

**Cellular Uptake Study.** Cells were seeded on a 12-well plate with a glass cover slip at the bottom of each well ($5 \times 10^4$ cells/well) and incubated at 37 °C with 5% $CO_2$ for 24 h. The medium was replaced with free DOX and DOX-loaded nanoparticles (2 $\mu$g/mL of DOX) for another 4 h incubation. The cells were washed three times with PBS and fixed by 4% paraformaldehyde for 20 min at room temperature. After washing three times with PBS, the cells were stained by 4′,6-diamidino-2-phenylindole for 10 min and kept in PBS. Confocal microscopy was used to visualize and record images.



DOI: 10.1021/acsomega.7b00367
*ACS Omega* 2017, 2, 3399−3405

**Scheme 1. Synthetic Scheme for the Preparation of PNIPAM-*b*-PMAA-Grafted Silica Nanoparticles**

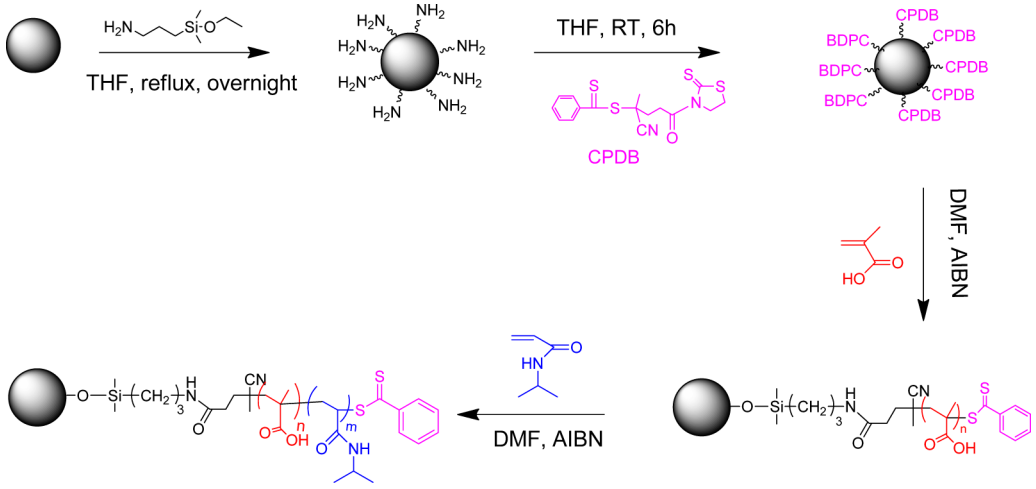


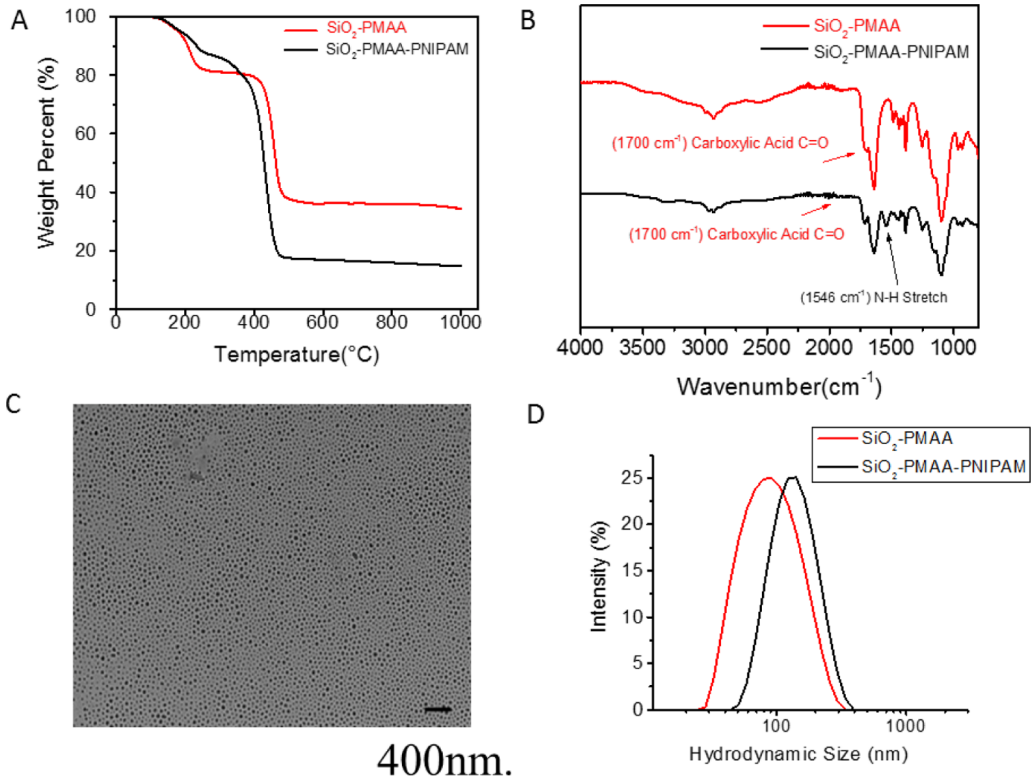


**Figure 1.** Characterization of $SiO_2$-PMAA and $SiO_2$-PMAA-*b*-PNIPAM nanoparticles. (A) TGA. (B) Infrared spectra. (C) Transmission electron microscopy (TEM) of aqueous solution of $SiO_2$-PMAA-*b*-PNIPAM particles. (D) Hydrodynamic size determined by dynamic light scattering (DLS).

## RESULTS AND DISCUSSION

The strategy for the preparation of PNIPAM-*b*-PMAA-grafted silica nanoparticles is shown in Scheme 1. Two separate SI-RAFT polymerizations were conducted sequentially to build well-defined diblock copolymers onto 15 nm silica nanoparticle surfaces. The polymerization of the first block was conducted employing a ratio among species of [MAA]/[RAFT]/[AIBN] = 1000:1:0.1 at 65 °C. The monomer conversion, followed by $^1$H NMR, was found to be 18.5% after 2.5 h, indicating 185 repeat units of each PMAA chain on average (Figure S1). Thermogravimetric analysis (TGA) showed that the grafted polymer accounted for about 70 wt % of the nanoparticles. The PMAA-grafted nanoparticles were washed several times by diethyl ether to remove excess monomer and initiator. The polymerization of the second block was conducted using NIPAM as monomer with a ratio among species [NIPAM]/[RAFT]/[AIBN] = 1000:1:0.1 in DMF at 65 °C. The reaction was followed by $^1$H NMR spectroscopy to calculate the conversion (Figure S2). The final product was characterized to be $SiO_2$-$PMAA_{185}$-*b*-$PNIPAM_{573}$, where the subscripts represent the number of repeat units. TGA showed that the total polymer content was ~90% (Figure 1A). Fourier transform infrared spectroscopy (Figure 1B) of the nanoparticles confirmed the existence of a block copolymer. The presence of a broad peak at ~3400 $cm^{-1}$ ascribed to hydroxyl groups and



DOI: 10.1021/acsomega.7b00367
ACS Omega 2017, 2, 3399−3405

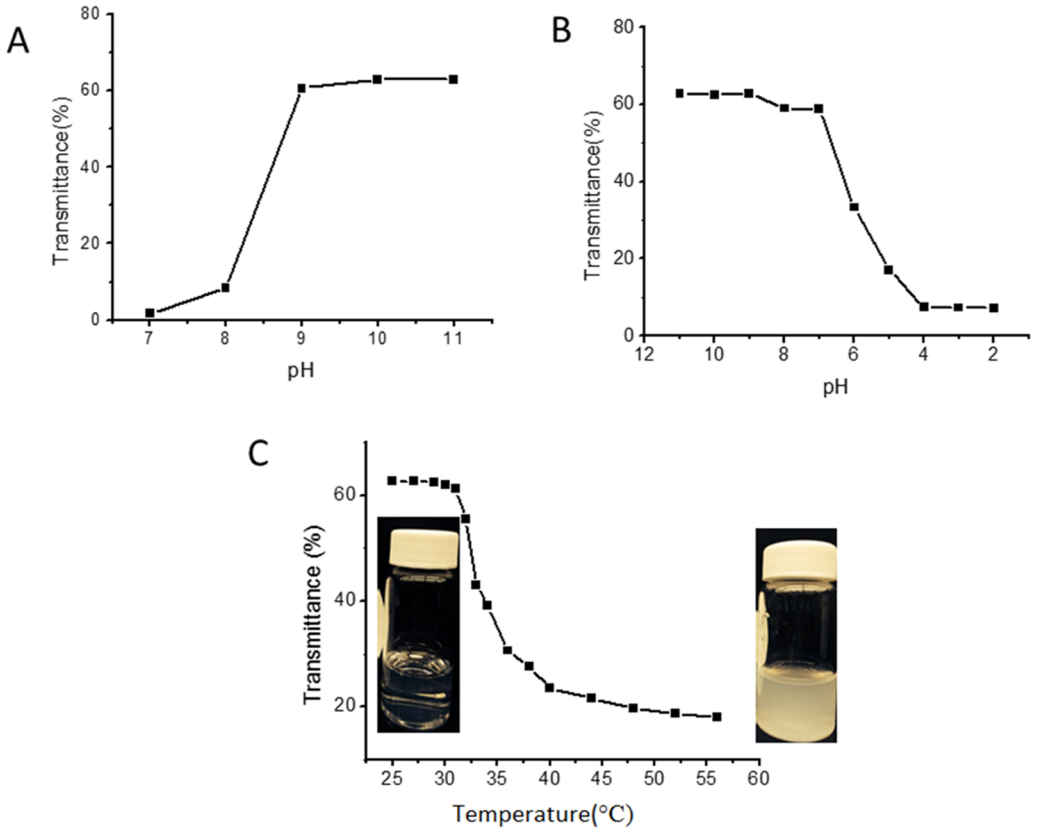


**Figure 2.** Transmittance curves with base (A) and acid (B) additions to aqueous $SiO_2$-PMAA-*b*-PNIPAM solution. (C) Transmittance change at 300 nm with increasing temperature of a $SiO_2$-PMAA-*b*-PNIPAM solution at pH 7.

the strong absorption at ~1700 $cm^{-1}$ corresponding to C═O double bonds confirmed the successful attachment of the PMAA chains. An additional peak at ~1546 $cm^{-1}$ appeared after the second polymerization, which is reported to be a characteristic of N−H stretching,[25] confirmed the attachment of the PNIPAM block.

**TEM and DLS Studies.** Both of the PMAA-grafted and PMAA-*b*-PNIAPM-grafted silica nanoparticles could be readily dispersed in water at neutral pH and room temperature. The individual nature of the nanoparticles was confirmed using TEM, as shown in Figure 1C. The hydrodynamic diameter of the particles was measured by DLS (Figure 1D). PMAA-$SiO_2$ particles had a *Z*-average diameter of 79.99 nm with a narrow PDI of 0.168, indicating that the particles were uniform in size. The $SiO_2$-PMAA-*b*-PNIPAM particles were found to have a *Z*-average diameter of 122.9 nm, ~43 nm larger than $SiO_2$-PMAA particles, which further confirmed the successful attachment of the second block.

**Double Stimuli-Responsive Properties of $SiO_2$-PMAA-*b*-PNIPAM.** The as-prepared $SiO_2$-PMAA-*b*-PNIPAM nanoparticles in aqueous solution responded to both pH and temperature as expected. Initial mixing between the dried nanoparticles and DI water resulted in a slightly turbid solution, which cleared up immediately after addition of a small amount of a base to break the interpolymer hydrogen bonding.[26,27] Acid (1 equiv) was then added to adjust the pH back to neutral, and no aggregation occurred during the process. The turbidity change during the process was measured by UV−vis at 300 nm, as shown in Figure 2.

The thermal responsive behavior of the $SiO_2$-PMAA-*b*-PNIPAM particles was investigated using both optical spectroscopy and DLS. A transparent solution of particles dispersed in water at pH 7 was heated from room temperature to 57 °C. As shown in Figure 2C, the transmittance decreased dramatically at 32 °C, corresponding to the LCST of PNIPAM, indicating the formation of aggregates due to decreased solubility of the PNIPAM corona. The aggregation of particles with increasing temperature was also monitored using DLS. At room temperature, only one sharp peak was found corresponding to monodispersed particles. When the temperature was increased above 32 °C, a second peak centered at approximately 600 nm appeared, which represented the formation of aggregates (Figure S3).

**In Vitro Drug Release of DOX.** DOX is a widely studied model drug that conjugates well with negatively charged polymers via electrostatic interactions.[22] At neutral pH, DOX molecules, with p$K_a$ 8.6, are positively charged, which leads to a strong interaction with negatively charged PMAA polymer chains. The LC and EE of DOX in $SiO_2$-PMAA-*b*-PNIPAM were calculated to be 21.2 and 89.8%, respectively, when the weight percent of initial DOX feeding was 30% (Table 1).[28] Compared to those of other core−shell type drug carriers,[29−32] the ones prepared in this work showed significantly higher EE and LC. At least two factors contributed to this unusually high

**Table 1. LC and EE with Different Feed Ratios**

| DOX/particles weight ratio | LC (%) | EE (%) |
|---|---|---|
| 3:10 | 21.2 ± 0.2 | 89.8 ± 2.6 |
| 5:10 | 31.4 ± 0.4 | 91.6 ± 2.4 |
| 7.5:10 | 40.3 ± 0.2 | 90.2 ± 0.8 |
| 10:10 | 49.4 ± 0.3 | 97.5 ± 1.2 |



DOI: 10.1021/acsomega.7b00367
*ACS Omega* 2017, 2, 3399−3405

amount of DOX loading. First, high polymer content was achieved because of the small size of the cores and high graft density. TGA results showed that 90 wt % of the nanoparticles was polymer, whereas the silica cores accounted for only 10 wt %. Second, once DOX was loaded onto the PMAA chains, the outer PNIPAM layer will act as a shield to prevent the loaded drug from escaping. An even higher LC could be achieved with 50, 75, and 100% feed ratios (Table 1). The in vitro DOX release profile from $SiO_2$-PMAA-*b*-PNIPAM particles (3:10 feed ratio) under different conditions is shown in Figure 3. The

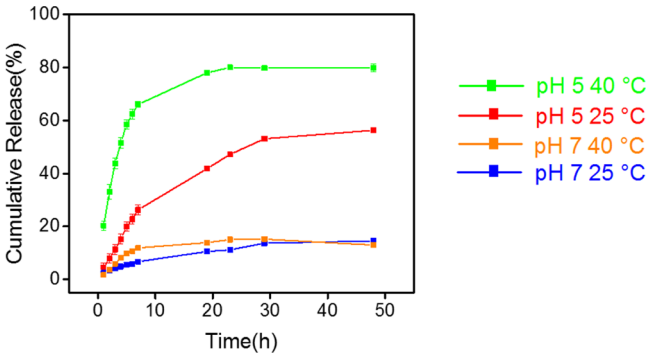


**Figure 3.** In vitro DOX release profile at different pHs and temperatures.

release performance was studied at both physiological pH (7.4) and lysosomal pH (5.0) conditions at temperatures of 25 and 40 °C. The release profiles revealed that release rates depended on both pH and temperature. Only limited amounts of loaded DOX were released at pH 7, regardless of temperature; however, under acidic conditions, significant amounts of DOX could be released during the same period of time.[33] Approximately 50% of the loaded drugs were released at pH 5 and 25 °C, whereas more than 80% were released at pH 5 and 40 °C. The best release result was obtained under conditions of acidic pH and elevated temperature, which is the typical environment for cancer cells. The mechanism behind the differences in release rates is depicted in Scheme 2. The electrostatic attraction between negatively charged polymer and positively charge DOX prevented significant release at neutral pH. However, under acidic conditions, protonation of the carboxylic acid groups of PMAA weakened the electrostatic interaction, enhancing DOX release. The release rate was further boosted by increasing temperature above the LCST, which collapsed the PNIPAM chains and caused the nanoparticles to agglomerate. The agglomeration process greatly reduced interparticle spacing and squeezed out DOX at a higher rate. This temperature-controlled agglomeration behavior also allowed particles to circulate without a significant drug loss but precipitate and concentrate at places at elevated temperatures. It is worth noting that the slight decrease of DOX after 30 h for pH 7 and 40 °C was because of the thermal degradation of DOX at elevated temperature.[34]

**Cell Viability Assay.** In vitro cytotoxicity of $SiO_2$-PMAA-*b*-PNIPAM nanoparticles, DOX-loaded $SiO_2$-PMAA-*b*-PNIPAM nanoparticles, and free DOX were studied on Hela cells by a CellTiter-Blue assay. Figure 4 shows the cytotoxicity profile of Hela cells incubated with various concentrations of $SiO_2$-PMAA-*b*-PNIPAM nanoparticles. These control nanoparticles showed no significant toxic effects up to 200 $\mu$g/mL. In contrast, DOX-loaded nanoparticles caused significant death of Hela cells at low concentration. Moreover, DOX-loaded nanoparticles exhibited a higher cytotoxic effect than free DOX of the same dose at low concentration. This difference in drug efficiency is most pronounced in the range of 5−10 $\mu$g/mL, where DOX-loaded nanoparticles resulted in 47% less cell viability for Hela cells compared to free DOX. This enhanced drug efficiency may be caused by the locally high concentration effect.[35]

**Cell Uptake.** Hela cells were incubated with free DOX and DOX-loaded nanoparticles at 37 °C. Figure 5 shows that after 4 h, red fluorescence was observed around the nuclei of Hela cells in both cases, indicating that the $SiO_2$-PMAA-*b*-PNIPAM nanoparticles are capable of internalizing into the nuclei of cancer cells.

**Scheme 2. Mechanism of Stimuli-Responsive Drug Release**

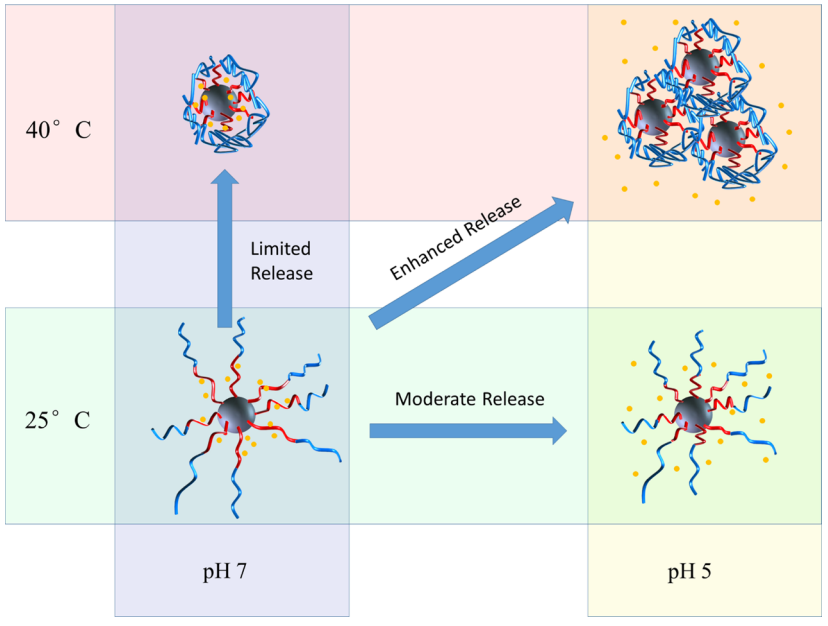




DOI: 10.1021/acsomega.7b00367
ACS Omega 2017, 2, 3399−3405

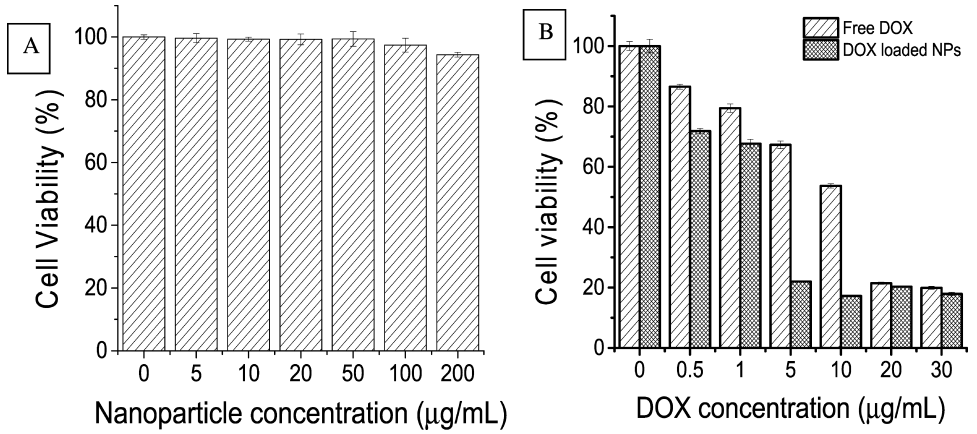


**Figure 4.** Relative cell viabilities of HeLa cells incubated with different concentrations of (A) $SiO_2$-PMAA-*b*-PNIPAM nanoparticles and (B) free DOX and DOX-loaded $SiO_2$-PMAA-*b*-PNIPAM nanoparticles.

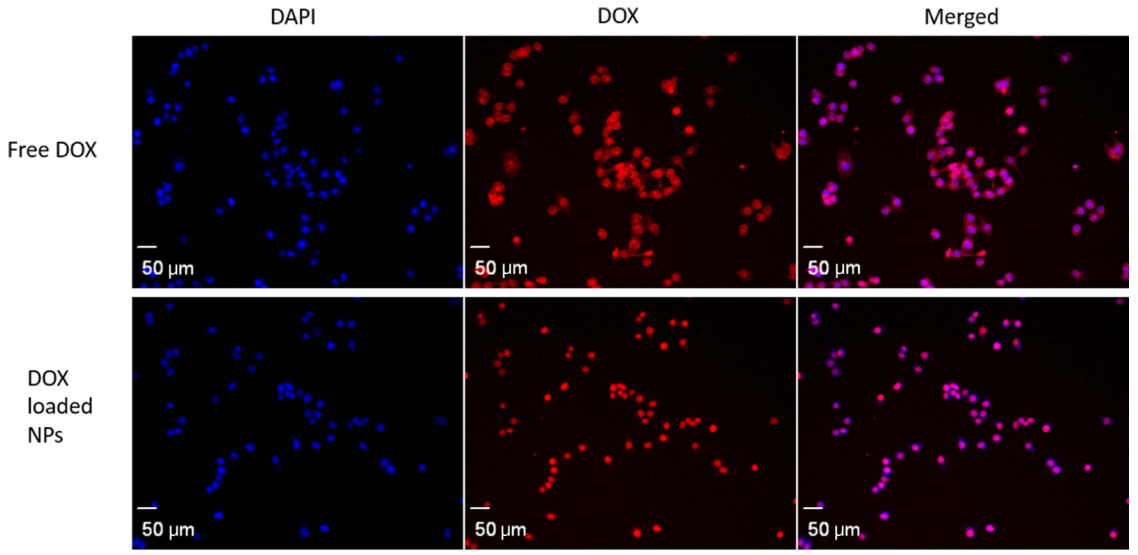


**Figure 5.** Cellular uptake analysis by confocal microscopy.

## CONCLUSIONS

In this study, we demonstrated the successful attachment of PMAA-*b*-PNIPAM block copolymers onto silica nanoparticles with a high grafting density using SI-RAFT polymerization. The resulting nanoparticles exhibited responses to both pH and temperature in aqueous solution as they dispersed individually at high pH and low temperature but agglomerated and precipitated out under acidic conditions or at elevated temperatures. DOX was loaded onto these nanoparticles with a very high LC and EE, and the release rate was found to be controlled by environmental pH and temperature. Cytotoxicity studies showed that the DOX-loaded $SiO_2$-PMAA-*b*-PNIPAM nanoparticles are highly active against Hela cells and more effective than free DOX of an equivalent dose. The integration of these functionalities may result in $SiO_2$-PMAA-*b*-PNIPAM nanoparticles becoming ideal drug carriers for anticancer drug delivery and biomedical applications.

## ASSOCIATED CONTENT

### Supporting Information

The Supporting Information is available free of charge on the ACS Publications website at DOI: 10.1021/acsomega.7b00367. NMR, DLS, and TEM images of grafted nanoparticles; calibration curve of DOX (PDF)

## AUTHOR INFORMATION

### Corresponding Author

*E-mail: benice@sc.edu.

### ORCID

Yang Zheng: 0000-0002-1960-5865
Qian Wang: 0000-0002-2149-384X
Brian C. Benicewicz: 0000-0003-4130-1232

### Notes

The authors declare no competing financial interest.

## ACKNOWLEDGMENTS

B.C.B. acknowledges financial support from the South Carolina SmartState Centers of Economic Excellence program. Q.W. acknowledges support from USC NSF CHE-1307319.

## REFERENCES

(1) Miller, K. P.; Wang, L.; Benicewicz, B. C.; Decho, A. W. Inorganic nanoparticles engineered to attack bacteria. *Chem. Soc. Rev.* **2015**, *44*, 7787−7807.



DOI: 10.1021/acsomega.7b00367
*ACS Omega* 2017, 2, 3399−3405

(2) Kumar, S. K.; Jouault, N.; Benicewicz, B.; Neely, T. Nanocomposites with Polymer Grafted Nanoparticles. *Macromolecules* **2013**, *46*, 3199−3214.
(3) Erathodiyil, N.; Ying, J. Y. Functionalization of Inorganic Nanoparticles for Bioimaging Applications. *Acc. Chem. Res.* **2011**, *44*, 925−935.
(4) Liong, M.; Lu, J.; Kovochich, M.; Xia, T.; Ruehm, S. G.; Nel, A. E.; Tamanoi, F.; Zink, J. I. Multifunctional Inorganic Nanoparticles for Imaging, Targeting, and Drug Delivery. *ACS Nano* **2008**, *2*, 889−896.
(5) Li, J.; Wang, L.; Benicewicz, B. C. Synthesis of Janus Nanoparticles via a Combination of the Reversible Click Reaction and "Grafting to" Strategies. *Langmuir* **2013**, *29*, 11547−11553.
(6) Li, C.; Han, J.; Ryu, C. Y.; Benicewicz, B. C. A Versatile Method To Prepare RAFT Agent Anchored Substrates and the Preparation of PMMA Grafted Nanoparticles. *Macromolecules* **2006**, *39*, 3175−3183.
(7) Li, Y.; Krentz, T. M.; Wang, L.; Benicewicz, B. C.; Schadler, L. S. Ligand Engineering of Polymer Nanocomposites: From the Simple to the Complex. *ACS Appl. Mater. Interfaces* **2014**, *6*, 6005−6021.
(8) Qiao, Y.; Islam, M. S.; Wang, L.; Yan, Y.; Zhang, J.; Benicewicz, B. C.; Ploehn, H. J.; Tang, C. Thiophene Polymer-Grafted Barium Titanate Nanoparticles toward Nanodielectric Composites. *Chem. Mater.* **2014**, *26*, 5319−5326.
(9) Natarajan, B.; Neely, T.; Rungta, A.; Benicewicz, B. C.; Schadler, L. S. Thermomechanical Properties of Bimodal Brush Modified Nanoparticle Composites. *Macromolecules* **2013**, *46*, 4909−4918.
(10) Li, Y.; Wang, L.; Natarajan, B.; Tao, P.; Benicewicz, B. C.; Ullal, C.; Schadler, L. S. Bimodal "matrix-free" polymer nanocomposites. *RSC Adv.* **2015**, *5*, 14788−14795.
(11) Zheng, Y.; Huang, Y.; Abbas, Z. M.; Benicewicz, B. C. Surface-initiated polymerization-induced self-assembly of bimodal polymer-grafted silica nanoparticles towards hybrid assemblies in one step. *Polym. Chem.* **2016**, *7*, 5347−5350.
(12) Zheng, Y.; Huang, Y.; Abbas, Z. M.; Benicewicz, B. C. One-pot synthesis of inorganic nanoparticle vesicles via surface-initiated polymerization-induced self-assembly. *Polym. Chem.* **2017**, *8*, 370−374.
(13) Wei, M.; Gao, Y.; Li, X.; Serpe, M. J. Stimuli-responsive polymers and their applications. *Polym. Chem.* **2017**, *8*, 127−143.
(14) Liu, F.; Urban, M. W. Recent advances and challenges in designing stimuli-responsive polymers. *Prog. Polym. Sci.* **2010**, *35*, 3−23.
(15) Yang, Y.; Ding, X.; Urban, M. W. Chemical and physical aspects of self-healing materials. *Prog. Polym. Sci.* **2015**, *49−50*, 34−59.
(16) Li, Q.-L.; Xu, S.-H.; Zhou, H.; Wang, X.; Dong, B.; Gao, H.; Tang, J.; Yang, Y.-W. pH and Glutathione Dual-Responsive Dynamic Cross-Linked Supramolecular Network on Mesoporous Silica Nanoparticles for Controlled Anticancer Drug Release. *ACS Appl. Mater. Interfaces* **2015**, *7*, 28656−28664.
(17) Zhou, H.; Wang, X.; Tang, J.; Yang, Y.-W. Tuning the growth, crosslinking, and gating effect of disulfide-containing PGMAs on the surfaces of mesoporous silica nanoparticles for redox/pH dual-controlled cargo release. *Polym. Chem.* **2016**, *7*, 2171−2179.
(18) Zhou, H.; Wang, X.; Tang, J.; Yang, Y.-W. Surface Immobilization of pH-Responsive Polymer Brushes on Mesoporous Silica Nanoparticles by Enzyme Mimetic Catalytic ATRP for Controlled Cargo Release. *Polymers* **2016**, *8*, No. 277.
(19) Cash, B. M.; Wang, L.; Benicewicz, B. C. The preparation and characterization of carboxylic acid-coated silica nanoparticles. *J. Polym. Sci., Part A: Polym. Chem.* **2012**, *50*, 2533−2540.
(20) Li, Q.-L.; Gu, W.-X.; Gao, H.; Yang, Y.-W. Self-assembly and applications of poly(glycidyl methacrylate)s and their derivatives. *Chem. Commun.* **2014**, *50*, 13201−13215.
(21) Schmaljohann, D. Thermo- and pH-responsive polymers in drug delivery. *Adv. Drug Delivery Rev.* **2006**, *58*, 1655−1670.
(22) Ma, W.-F.; Wu, K.-Y.; Tang, J.; Li, D.; Wei, C.; Guo, J.; Wang, S.-L.; Wang, C.-C. Magnetic drug carrier with a smart pH-responsive polymer network shell for controlled delivery of doxorubicin. *J. Mater. Chem.* **2012**, *22*, 15206−15214.
(23) Xu, Z.; Wang, D.; Guan, M.; Liu, X.; Yang, Y.; Wei, D.; Zhao, C.; Zhang, H. Photoluminescent Silicon Nanocrystal-Based Multifunctional Carrier for pH-Regulated Drug Delivery. *ACS Appl. Mater. Interfaces* **2012**, *4*, 3424−3431.
(24) Wang, L.; Benicewicz, B. C. Synthesis and Characterization of Dye-Labeled Poly(methacrylic acid) Grafted Silica Nanoparticles. *ACS Macro Lett.* **2013**, *2*, 173−176.
(25) Yang, Y.; Yan, X.; Cui, Y.; He, Q.; Li, D.; Wang, A.; Fei, J.; Li, J. Preparation of polymer-coated mesoporous silica nanoparticles used for cellular imaging by a "graft-from" method. *J. Mater. Chem.* **2008**, *18*, 5731−5737.
(26) Teresa Garay, M.; Cristina Llamas, M.; Iglesias, E. Study of polymer-polymer complexes and blends of poly(N-isopropylacrylamide) with poly(carboxylic acid): 1. Poly(acrylic acid) and poly(methacrylic acid). *Polymer* **1997**, *38*, 5091−5096.
(27) Ruiz-Rubio, L.; Laza, J.; Pérez, L.; Rioja, N.; Bilbao, E. Polymer−polymer complexes of poly(N-isopropylacrylamide) and poly(N,N-diethylacrylamide) with poly(carboxylic acids): a comparative study. *Colloid Polym. Sci.* **2014**, *292*, 423−430.
(28) Sahoo, B.; Devi, K. S. P.; Banerjee, R.; Maiti, T. K.; Pramanik, P.; Dhara, D. Thermal and pH Responsive Polymer-Tethered Multifunctional Magnetic Nanoparticles for Targeted Delivery of Anticancer Drug. *ACS Appl. Mater. Interfaces* **2013**, *5*, 3884−3893.
(29) Chang, B.; Sha, X.; Guo, J.; Jiao, Y.; Wang, C.; Yang, W. Thermo and pH dual responsive, polymer shell coated, magnetic mesoporous silica nanoparticles for controlled drug release. *J. Mater. Chem.* **2011**, *21*, 9239−9247.
(30) Hu, X.; Hao, X.; Wu, Y.; Zhang, J.; Zhang, X.; Wang, P. C.; Zou, G.; Liang, X.-J. Multifunctional hybrid silica nanoparticles for controlled doxorubicin loading and release with thermal and pH dual response. *J. Mater. Chem. B* **2013**, *1*, 1109−1118.
(31) Chen, L.; Peng, Z.; Zeng, Z.; She, Y.; Wei, J.; Chen, Y. Hairy polymeric nanocapsules with ph-responsive shell and thermoresponsive brushes: Tunable permeability for controlled release of water-soluble drugs. *J. Polym. Sci., Part A: Polym. Chem.* **2014**, *52*, 2202−2216.
(32) Tan, L.; Liu, J.; Zhou, W.; Wei, J.; Peng, Z. A novel thermal and pH responsive drug delivery system based on ZnO@PNIPAM hybrid nanoparticles. *Mater. Sci. Eng., C* **2014**, *45*, 524−529.
(33) Tian, B.; Liu, S.; Lu, W.; Jin, L.; Li, Q.; Shi, Y.; Li, C.; Wang, Z.; Du, Y. Construction of pH-responsive and up-conversion luminescent NaYF4:Yb3+/Er3+@SiO2@PMAA nanocomposite for colon targeted drug delivery. *Sci. Rep.* **2016**, *6*, No. 21335.
(34) Beijnen, J.; Van der Houwen, O.; Underberg, W. Aspects of the degradation kinetics of doxorubicin in aqueous solution. *Int. J. Pharm.* **1986**, *32*, 123−131.
(35) Wang, L.; Chen, Y. P.; Miller, K. P.; Cash, B. M.; Jones, S.; Glenn, S.; Benicewicz, B. C.; Decho, A. W. Functionalised nanoparticles complexed with antibiotic efficiently kill MRSA and other bacteria. *Chem. Commun.* **2014**, *50*, 12030−12033.


DOI: 10.1021/acsomega.7b00367
*ACS Omega* 2017, 2, 3399−3405